

RESEARCH ARTICLE

Lower miR-26a levels in breastmilk affect gene expression in adipose tissue of offspring

Catalina A. Pomar^{1,2,3}  | Francisca Serra^{1,2,3}  | Andreu Palou^{1,2,3}  | Juana Sánchez^{1,2,3} 

¹Laboratory of Molecular Biology, Nutrition and Biotechnology (Nutrigenomics, Biomarkers and Risk Evaluation), University of the Balearic Islands, Palma, Spain

²Instituto de Investigación Sanitaria Illes Balears, IdISBa, Palma, Spain

³CIBER Fisiopatología de la Obesidad y Nutrición (CIBEROBN), Instituto de Salud Carlos III (ISCIII), Madrid, Spain

Correspondence

Francisca Serra, Laboratory of Molecular Biology, Nutrition and Biotechnology (Nutrigenomics, Biomarkers and Risk Evaluation), University of the Balearic Islands, Edifici Mateu Orfila, Carretera de Valldemossa Km 7.5, Palma 07122, Spain.

Email: francisca.serra@uib.es

Funding information

MINECO | Instituto de Salud Carlos III (ISCIII), Grant/Award Number: PI17/01614

Abstract

Breastmilk miRNAs may act as epigenetic regulators of metabolism and energy homeostasis in offspring. Here, we aimed to investigate the regulatory effects of miR-26a on adipose tissue development. First, the 3T3-L1 cell model was used to identify putative target genes for miR-26a. Then, target genes were analysed in adipose tissue of offspring from dams that supplied lower levels of breastmilk miR-26a to determine whether miR-26a milk concentration might have a long-lasting impact on adipose tissue in the progeny. In the in vitro model, both over- and under-expression of miR-26a were induced by transfecting into 3T3-L1 with miR-26a mimic and inhibitor. Array analysis was performed after induction of miR-26a to ascertain the impact on mRNA target genes and influence of differentiation status. Focusing on genes related to adipose tissue development, transfection with miR-26a mimic reduced the expression of *Pten*, *Hmga1*, *Stk11*, *Rb1*, and *Adam17* in both pre- and mature adipocytes. Data mostly confirmed the results found in the animal model. After weaning, descendants of cafeteria-fed dams breastfed with lower levels of miR-26a displayed greater expression of *Hmga1*, *Rb1*, and *Adam17* in retroperitoneal white adipose tissue in comparison with controls. Hence, alterations in the amount of miR-26a supplied through milk during lactation is able to alter the expression of target genes in the descendants and may affect adipose tissue development. Thus, milk miR-26a may act as an epigenetic regulator influencing early metabolic program in the progeny, which emerges as a relevant component of an optimal milk composition for correct development.

KEYWORDS

breastfeeding, breastmilk, milk's epigenetic regulators, miR-26a

Abbreviations: Adam17, ADAM metallopeptidase domain 17; DM, differentiation medium; Hmga1, high mobility group AT-hook 1; Hmga2, high mobility group AT-hook 2; MM, maintenance medium; NC, negative controls; O-C, offspring of control dams; O-CAF, offspring of cafeteria diet fed dams; Pten, phosphatase and tensin homolog; Ptk9, protein tyrosine kinase 9; Rb1, retinoblastoma 1; RT-qPCR, real-time quantitative polymerase chain reaction; Stk11, serine/threonine protein kinase 11.

This is an open access article under the terms of the Creative Commons Attribution-NonCommercial-NoDerivs License, which permits use and distribution in any medium, provided the original work is properly cited, the use is non-commercial and no modifications or adaptations are made.

© 2021 The Authors. *The FASEB Journal* published by Wiley Periodicals LLC on behalf of Federation of American Societies for Experimental Biology

1 | INTRODUCTION

The global incidence of obesity and obesity-related disorders, including diabetes, metabolic syndrome, and cardiovascular disease, has given rise to a demand for effective early therapeutic interventions. By assuming an average optimal composition of breastmilk, it is considered that breastfeeding represents optimal nutrition during immediate postnatal life and compared with infant formula feeding confers reliable protection against obesity in adult life.^{1–3} Thus, nutrition during development modulates infant metabolic programming. The mechanisms of metabolic programming are poorly characterized, but there is growing evidence that epigenetic mechanisms may facilitate developmental plasticity of the infant and affect the phenotype in later-life.^{4–6}

Breastmilk is a rich source of miRNAs⁷ which could act as milk epigenetic regulators.⁸ Evidence suggests that levels of specific miRNAs in human milk are modulated by maternal diet⁹ and maternal weight.^{10,11} However, the impact of maternal environment on specific changes in milk miRNA content and their potential involvement in metabolic programming in the offspring are not fully understood. Recently, our group has described that human breastmilk supply of specific miRNAs is affected by maternal overweight/obesity and may influence infant body mass index.¹¹ In this regard, the study of how breastmilk miRNA levels altered by maternal status could act as epigenetic factors and modulate both infant development and future health, is of great basic interest in the fields of nutrition and healthy growth and development. In this regard, we have shown that maternal consumption of a cafeteria diet throughout lactation in rats produces lasting effects on the metabolic health of offspring. Specifically, animals show greater fat accumulation, despite normalization of the diet after weaning.¹² Furthermore, maternal intake of an obesogenic diet during lactation promotes specific changes in breastmilk miRNA levels, specifically an increase in miR-222 levels and decrease in miR-200a and miR-26a levels in comparison with levels observed in control dams.¹³ Bearing in mind the outcomes observed in the offspring associated to these maternal inputs, it could be hypothesized that changes in these specific miRNAs, affected by maternal nutritional conditions, may play a role in adipose tissue development in the offspring.

Many studies have reviewed the role of miRNA as stimulators or inhibitors of murine and/or human adipocyte differentiation.^{14–16} Among others, a key player in adipocyte development is the miR-26 family, made up of miR-26a and miR-26b.¹⁷ Both, miR-26a and miR-26b are induced early during adipogenesis and are required for its progression.^{17,18} In addition, miR-26a expression

is downregulated in various obesity-associated organs of obese mouse models¹⁹ and miR-26b is also downregulated in visceral adipose tissue of diet-induced obese rats, ob/ob mice, and obese humans.²⁰ Noteworthy, mice lacking the highly conserved miR-26 miRNA family reveal a dramatic expansion of adipose tissue.²¹ In this regard, lower levels of miR-26a supplied through the breastmilk from cafeteria-fed dams¹³ could act by programming higher adipose tissue development in offspring. To test this hypothesis, in the present study we identified and confirmed *in vitro* direct mRNA targets of miR-26a and then analysed whether expression of these targets was altered early in adipose tissue of the offspring from dams who supplied lower levels of miR-26a through breastmilk. Results show that the amount of miR-26a supplied through milk during lactation alters the expression of target genes in the descendants and may affect adipose tissue development by acting as an epigenetic regulator.

2 | MATERIALS AND METHODS

2.1 | Experimental design at a glance

Detailed information of the methods used is described below. The workflow and experimental design of the study is depicted in Figure 1. First, 3T3-L1 confluent preadipocytes (day 0) were transfected with either a miR-26a mimic, a miR-26a inhibitor, or their respective negative controls (Mimic-NC or Inhibitor-NC). Cells were collected at day 2 and 8 to study the effect in both pre-adipocytes (d2) and mature adipocytes (d8). Transcriptomic analysis in a subset of pre- and mature cells transfected with miR-26a mimic and the respective NC were run to identify miR-26a target genes. Data processing was focused on the identification of miR-26a target genes fulfilling the following conditions: downregulated expression in cells transfected with miR-26a mimic, found to be significantly decreased in both pre- and mature adipocytes, and having predicted miR-26 binding sites (according to Targetscan7.2). Then, to better narrow-down the list a filter based on functionality was applied, focusing on genes with a well-known role in adipocyte development/differentiation that would represent a good proxy of biomarkers for miR-26a metabolic action.

Next step was devoted to confirming the role of the selected target mRNA derived from the array results. Therefore, the expression of selected genes/biomarkers was determined by real-time quantitative RT-polymerase chain reaction (RT-qPCR) in the whole set of *in vitro* samples, including cells transfected with the inhibitor of miR-26a and the respective NC. Finally, expression of the

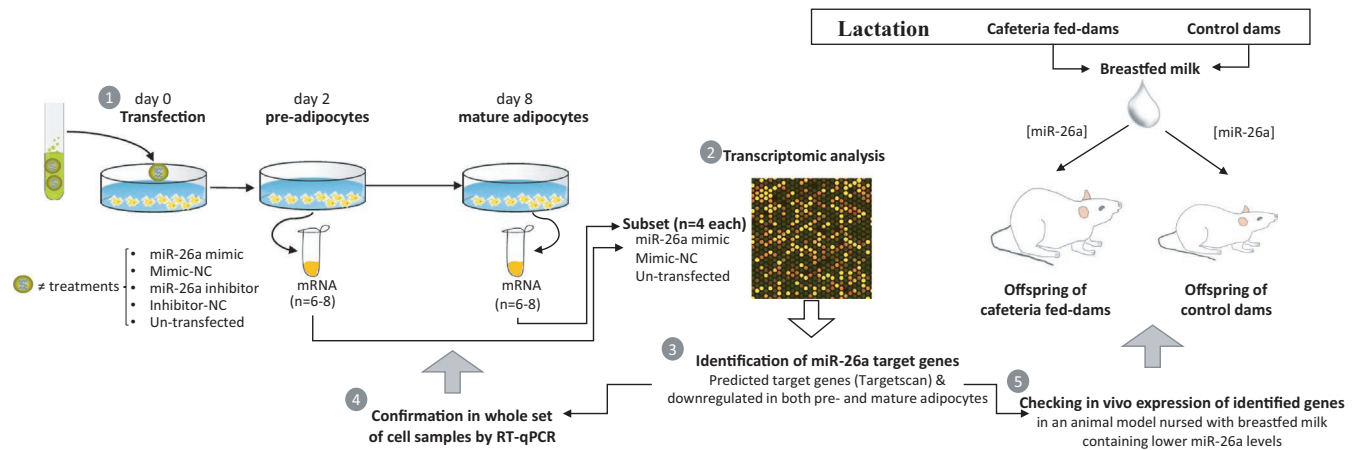


FIGURE 1 Summary of the workflow and the experimental design. NC, negative control; RT-qPCR, real-time quantitative RT-polymerase chain reaction

biomarkers for miR-26a metabolic action was assessed in a physiological animal model nursed during lactation with breastmilk providing a lower supply of miR-26a, in order to test in vivo effects of miR-26a suboptimal intake and to assess whether adipose tissue in offspring was showing altered gene expression that could explain the greater adiposity found in these animals. To get the physiological animal model providing suboptimal miR-26a in breastmilk, 3-month-old primiparous dams were exposed to cafeteria diet in addition to the standard chow during lactation from day 1 after delivery (cafeteria dams) whereas a matched group was kept under standard chow diet (control dams).^{12,13}

2.2 | Cell culture and differentiation

Murine 3T3-L1 fibroblasts were purchased from ZenBio and cultured in preadipocyte medium (Zenbio) at 37°C in 10% CO₂. To induce differentiation, cells were allowed to reach confluence and differentiation was induced after 48 h of confluence (day 0). At day 0, 3T3-L1 cells were cultured for 2 days in a differentiation medium (DM) containing 5 µg/ml insulin, 0.5 mmol/L 3-isobutyl-1-methyl-xantine, 0.5 µmol/l dexamethasone, 100 U/ml penicillin, 100 µg/ml streptomycin, and 10% fetal bovine serum (FBS) in Dulbecco's modified Eagle's medium-high glucose (DMEM) at 37°C, 8% CO₂, and saturated humidity. Then, the medium was replaced with maintenance medium (MM), containing DMEM with 5 µg/ml insulin, 100 U/ml penicillin, 100 µg/ml streptomycin, and 10% FBS. This medium was replaced every second day. Differentiation was monitored by morphological examination of cells for accumulation of lipid droplets; cells were considered fully differentiated after 8 days inducing differentiation.

2.3 | Transfection with miR-26a mimic and inhibitor

Cells were seeded into 24-well plates and transfection was performed at day 0. Lipofectamine RNAiMAX Reagent (Life Technologies, Madrid, Spain) was used according to the manufacturer's protocol. 3T3-L1 cells were transfected with either 50nM miR-26a mimic (MC10249, Life Technologies, Madrid, Spain), 50nM miR-26a inhibitor (MH10492, Life Technologies, Madrid, Spain), the respective negative controls (NC) (Mimic-NC and Inhibitor-NC, Life Technologies, Madrid, Spain), or positive controls of transfection performance (miR-1 and anti-miR let-7c, Life Technologies, Madrid, Spain) according to the manufacturer's instructions. In addition, un-transfected wells were followed as quality controls of the cell culture. After 48h of transfection, a set of wells were collected while the remaining were submitted to a change of medium, which was replaced by MM, and were then collected on day 8 of differentiation.

2.4 | Oil red O staining

Fat accumulation in 3T3-L1 cells was assessed by staining formalin-fixed cells with oil red O at day 8. Adipocytes were washed with phosphate buffered saline (PBS) and fixed with 10% formaldehyde in PBS for 1 h at room temperature. After fixation, cells were washed twice with water and then with 60% isopropanol and stained by incubation with oil red O (0.35 g oil red O in 100 ml isopropanol diluted with double distilled water [40:60] and filtrated) for 1 h. Cells were washed with water to remove unbound dye, visualized by light microscopy, and photographed. To quantify the intracellular lipid droplets, Oil Red O of stained cells was eluted with isopropanol and optical density measured at 500 nm wavelength.

2.5 | Total RNA isolation

Total RNA was extracted from 3T3-L1 cells at day 2 and day 8 of differentiation with TRI Reagent® (Sigma Aldrich Química SA, Madrid, Spain) according to the manufacturer's instructions. The integrity of total RNA was quantified in a NanoDrop ND-1000 spectrophotometer (NadroDrop Technologies Inc, Wilmington, DE, USA) and its integrity verified by agarose gel electrophoresis.

2.6 | miR-26a quantification

For specific miR-26a quantification, RNA was first reverse-transcribed and then amplified using the specific primers and probes provided with the TaqMan MicroRNA Reverse Transcription kit (Life Technologies, Madrid, Spain) in two steps, according to the manufacturer's protocol. Complementary DNA was synthesized by using 50 ng of total RNA and miRNA-specific RT primers (Assay ID: 000405) (Life Technologies, Madrid, Spain). The reactions were incubated at 16°C for 30 min, 42°C for 30 min, 85°C for 5 min, and then an indefinite hold at 4°C in an Applied Biosystems 2720 Thermal Cycler (Applied Biosystems, Madrid, Spain). Thereafter, miRNA expression was assessed using sequence specific primers from the TaqMan microRNA assays and Taqman Universal master mix (Life Technologies, Madrid, Spain), with the following real-time PCR schedule: 95°C for 10 min, 40 cycles of 95°C for 15 s, and 60°C for 60 s on the Applied Biosystems StepOnePlus Real-Time PCR Systems (Applied Biosystems, Madrid, Spain). Relative expression levels were quantified by the $2^{-\Delta\Delta Ct}$ method using U6 as a reference gene. In the case of tissue miR-26a determination, RNA was previously extracted in mammary gland as previously described²² and in retroperitoneal white adipose tissue as indicated in Section 2.8.

2.7 | Microarray processing and data analysis

RNA extracted from miR-26a mimic transfected cells at day 2 and day 8 (in each group: $n = 4$ wells from three separate experiments), the negative respective controls (Mimic-NC) and un-transfected cells were processed for microarray analysis. Quality control of samples was assessed with the Agilent 2100 Bioanalyzer with RNA 6000 Nano chips (Agilent Technologies, Barcelona, Spain). All samples had a RIN number > 9 . Microarray processing was performed using Mouse GE 8x60K Microarray according to the manufacturer's protocol (Agilent Technologies, Barcelona, Spain). Quality control checking and microarray processing

were carried out by the “Servicio de Genómica y Genética Traslacional” from the “Centro de Investigación Príncipe Felipe” (Valencia, Spain). Background correction of the files with the raw data was performed following the Agilent methodology. Subsequently, the signal intensity of the different arrays was standardized by quantile normalization. For the probes that pointed to the same gene, their median expression was calculated, summarizing the information in a single identifier. Differential expression was carried out using the moderate t-statistic of the Limma package. To minimize the number of false positives, p-values were adjusted using the method proposed by Benjamini-Hochberg. To test the effect of transfection with the miR-26a mimic, the following contrast was made: miR-26a mimic versus Mimic-NC on day 2 (preadipocytes) and on day 8 (mature adipocytes) and fold change was calculated. Analysis of signaling routes was done with HiPathia.²³ A contrast was made with Limma to compare the activation levels of each sub-route between two experimental groups of interest, and thus check whether the route had been activated or inhibited.

2.8 | RT-qPCR analysis

For RT-qPCR analysis, 0.2 μg of total RNA from cultured cells was used for reverse transcription by using the iScript™ cDNA synthesis kit (Bio-Rad Laboratories, SA, Madrid, Spain) according to the manufacturer's protocol. Real-time PCR was performed using the Applied Biosystems StepOnePlus™ Real-Time PCR Systems (Applied Biosystems, Madrid, Spain) with Power SYBER Green PCR Master Mix (Life Technologies, Madrid, Spain). Each PCR was performed from 1/10 dilution of the cDNA product and forward and reverse primers (5 μM each) (Sigma Aldrich Química SA, Madrid, Spain). After an initial Taq polymerase activation at 95°C for 10 min, PCR was performed using 40 two-temperature cycles with the following cycling conditions: 95°C for 15 s and 60°C for 1 min. Threshold cycle (Ct) values were calculated by StepOne Software v2.3 and the relative mRNA expression of each gene was expressed as a percentage of control cells, using the $2^{-\Delta\Delta Ct}$ method. The expression of β -actin was homogeneous among the different groups and was thus used as the reference gene.

2.9 | Gene expression analysis of miR-26a selected target genes in offspring of cafeteria-fed dams

Expression of mRNA of selected genes (identified by microarray) was analysed in retroperitoneal white adipose

tissue of offspring from dams fed a cafeteria diet during lactation belonging to a cohort of animals previously characterized in detail.¹² Tissue was collected after weaning at postnatal day 22. Total RNA extraction was performed using Tripure Reagent (Roche Diagnostic GmbH, Mannheim, Germany) according to the instructions of the manufacturer. Total RNA was quantified in a NanoDrop ND-1000 spectrophotometer (NadroDrop Technologies Inc, Wilmington, DE, USA) and its integrity verified by agarose gel electrophoresis. qRT-PCR was used to measure mRNA expression levels of the selected genes following the protocol described in the above Section 2.7. Gene expression levels were normalized using guanosine diphosphate dissociation inhibitor 1 (Gdi1) mRNA as the housekeeping gene.

2.10 | Statistical analysis

In cell culture experiments, values are presented as the mean \pm SEM from three separate experiments ($n = 6$ – 10 wells in each group). In the animal model approach, data are expressed as the mean \pm SEM ($n = 16$ – 20 animals in each group). The statistical analysis of microarray data is described in detail in the previous section (microarray data analysis). Single comparisons were assessed by Mann–Whitney U test for the cell experiments ($n < 10$) and by Student's *t*-test in animal model data ($n > 10$). Unless stated otherwise, $p < .05$ was defined as the threshold of significance. Statistics were computed with SPSS Statistics 21.0 (SPSS, Chicago, IL, USA).

3 | RESULTS

3.1 | Evaluation of miRNA transfection in 3T3-L1 cells

To assess the performance of miRNA transfection, two quality controls were performed. 3T3-L1 cells transfected with miR-1 were used as a positive control of miRNA transfection aiming to mimic the down regulation on a target gene associated to the delivery of miRNA. The activity of miR-1 was monitored through the gene silencing of protein tyrosine kinase 9 (*Ptk9*), which resulted in a significant reduction in *Ptk9* mRNA levels, 40% and 43% at day 2 and 8 respectively (Supporting Information Figure S1).

To test the performance of transfection using miRNA inhibitors, 3T3-L1 cells transfected with anti-miR let-7c were used as the functional control, aiming to block the action of the specific endogenous miRNA. Physiological miR let-7c downregulates the levels of the high mobility

group AT-hook 2 (*Hmga2*) mRNA, which corresponds to a ubiquitously expressed protein. Accordingly, anti-miR let-7c transfection was associated with an increase in *Hmga2* mRNA levels after 2 days of transfection (69%) which still remained (21%) at 8 days (Supporting Information Figure S1).

Delivery of both miRNA probes, either to activate miR-1 or to block miR let-7c activities, were effective in pre-adipocytes and showed sustained effects in mature adipocytes, suggesting that miRNA actions on target mRNA were maintained during adipocyte differentiation in the transfected cells.

3.2 | miR-26a impact on adipocyte differentiation

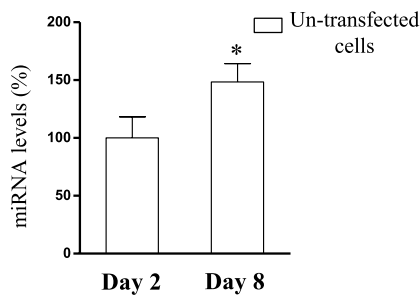
Endogenous miR-26a levels, checked in un-transfected 3T3-L1 cells, were greater (48%) in mature adipocytes (at day 8) than in pre-adipocytes (at day 2; Figure 2A), indicating that miR-26a expression is increased during adipocyte differentiation. As expected, cells transfected with the mimic miR-26a showed higher specific miR-26a expression compared to non-specific transfection effects (Mimic-NC) at day 2 ($\times 362$), which still was retained at day 8 ($\times 21$) (Figure 2B). Accordingly, cells transfected with the inhibitor of miR-26a displayed decreased levels of miR-26a in comparison with the corresponding control cells (Inhibitor-NC), at both day 2 and day 8 (45.5% and 41.5%, respectively), although the differences did not reach statistical significance (Figure 2B). No major differences were observed in the morphology of pre-adipocytes transfected with miR-26a mimic or the control (Figure 2C). However, on day 8, overexpression of miR-26a in mature adipocytes was suggestive of a greater degree of differentiation with larger lipid droplets accompanied by a tendency to show greater lipid accumulation (6%, $p = .06$) than in the respective control cells (Figure 2D).

3.3 | Overview of the effects of miR-26a mimic transfection on the cell transcriptome

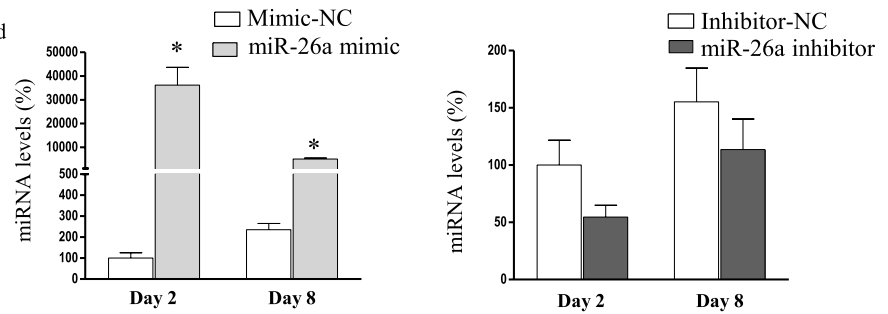
Transcriptomic analysis performed in cells after 2 days of transfection with miR-26a mimic showed a set of 2513 target genes that were differentially expressed (1219 genes under-expressed and 1294 overexpressed compared to Mimic-NC). Concerning the long-term impact of transfection on undifferentiated cells up to differentiated adipocytes, transfected cells still displayed a panel of target genes differentially expressed on day 8; 1193 mRNA species, 551 genes of which were under-expressed and 642

miR-26a effects on 3T3-L1 differentiation

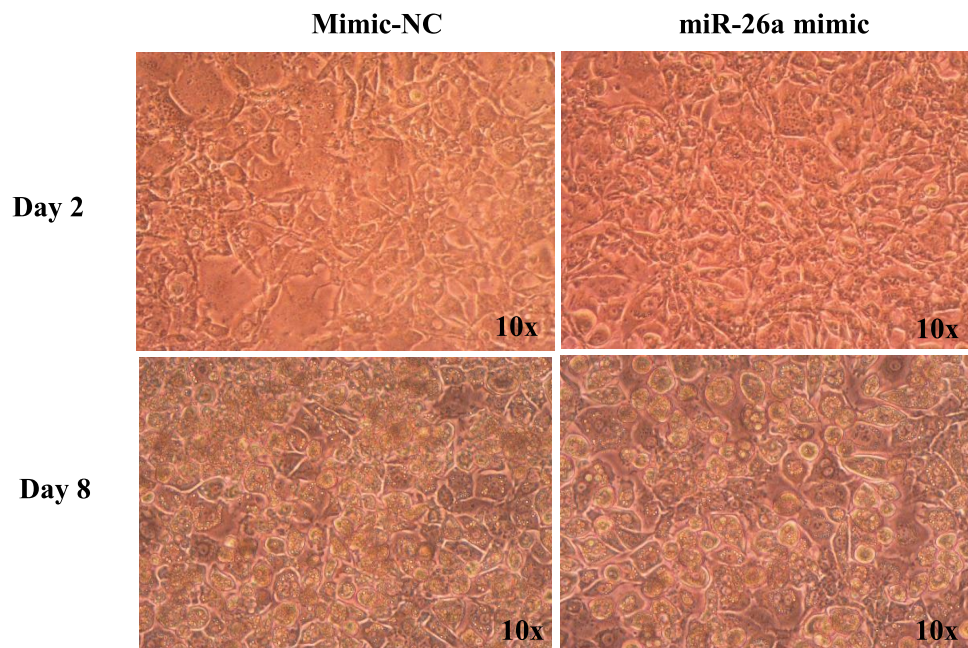
(A) miR-26a levels during adipocyte development



(B) miR-26a levels in transfected cells



(C) Representative photomicrographs of 3T3-L1 adipocytes at day 2 and 8 of differentiation



(D) Oil red O staining in miR-26a mimic transfected cells

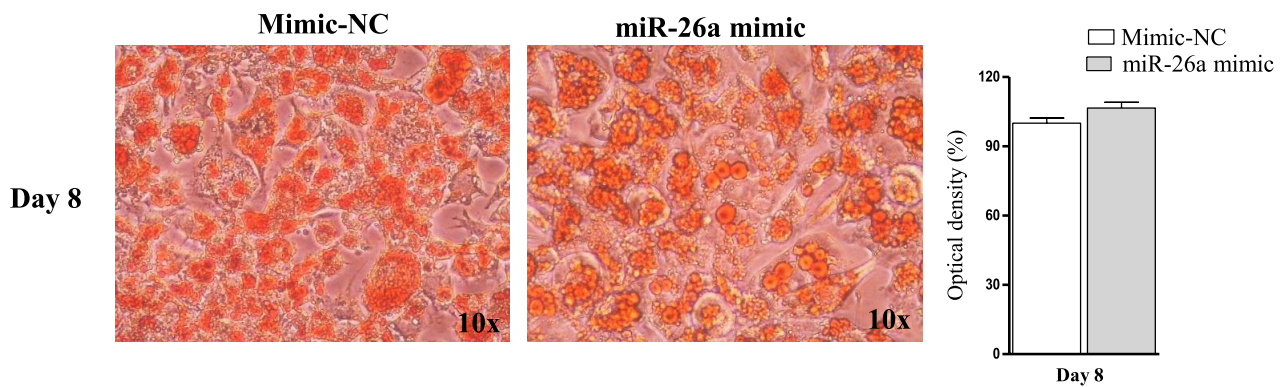


FIGURE 2 miR-26a during 3T3-L1 differentiation. (A) Expression level of miR-26a during cell differentiation under normal culture conditions. (B) Expression levels of miR-26a in cells transfected with the mimic and/or inhibitor. (C) Representative photomicrographs of 3T3-L1 adipocytes at day 2 and 8 of differentiation in cells transfected with the mimic of miR-26a at day 0 for 48 h. (D) Oil Red O staining on day 8 of 3T3-L1 adipocytes transfected with the mimic of miR-26a at day 0 for 48 h. Data are mean \pm SEM from three independent experiments ($n = 6-10$). Statistics: *different versus control cells ($p < .05$, Mann-Whitney U test)

overexpressed compared to Mimic-NC cells. These results suggest that transfection with a miR-26a mimic at the beginning of differentiation in 3T3-L1 cells impacts quite a high number of mRNA targets. The metabolic impact still remains, to a significant extent, during the progress toward differentiated cells.

The expression of a core group of 396 genes was significantly altered in the pre- and mature status of 3T3-L1 cells transfected with miR-26a mimic in comparison with their respective controls (Venn diagrams in Figure 3A). Results of gene expression of these genes are depicted in the heat map (Figure 3B). The unsupervised hierarchical clustering analysis of the samples revealed two levels of clustering: a first level highlighting the impact of the transfection with the miR26a-mimic and a second level showing the differentiation process. As expected, gene expression in pre-adipocytes clustered separated from mature adipocytes. In addition, the expression of these target genes separated the cells transfected with the miR-26a from those with the negative control, irrespective of the adipocyte differentiation status.

To delve further into the impact of miR-26a, further characterization was focused on genes with predicted miR-26a binding sites according to TargetScan7.2 (www.targetscan.org). Therefore, the database provided 54 predicted target mRNAs for miR-26a, able to interact with partially complementary sites in their 3'-untranslated regions (3'UTR) and to diminish protein output, either by mRNA destabilization or by inhibition of translation.²⁴ Of these, 50 were downregulated in both states of differentiation (Table 1). Phosphatase and tensin homolog (*Pten*) was the gene located at the top of the list, according to the aggregate PCT which is an estimate of the probability that a site is conserved due to miRNA targeting.²⁵ Furthermore, the list included other representatives of the PI3K-Akt pathway, such as Serine/Threonine protein kinase 11 (*Stk11*). Genes involved in adipogenesis (high mobility group AT-hook 1 (*Hmga1*) and retinoblastoma gene (*Rb1*)) and related functions (lipid transport, cell cycle, and regulation of cell size) were also recognized. Next, to obtain a holistic overview of the main signaling pathways involved, analysis with HiPathia²³ was performed with the changes produced in gene expression by mimic miR-26a. At day 2 of transfection, 160 pathways were affected (49.4% under-activated) and then, in mature adipocytes, 64 still remained different from control-transfected cells (36% under-activated). Of these, 25 pathways were significantly affected in both pre- and mature adipocytes and as seen under TargetScan constraints, the results highlighted representative members of the PI3K-Akt signaling pathway as highly statistically significant ones (Table 2).

Therefore, miR-26a mimic transfection induced a regulatory pattern of gene expression that drove around half of

the target genes under repression. The effect was observed at two days after transfection in pre-adipocytes and still remained in a subset of genes on day 8, in differentiated adipocytes. Specifically, 50 specific targets for miR-26a were consistently downregulated throughout the cell differentiation process, involving the PI3K-Akt signaling pathway to a relevant extent.

3.4 | Confirmation and validation of miR-26a impact on identified target genes

The next step was devoted to further confirming the microarray results by validating a subset of genes that could play a main role in adipocyte development and differentiation being targeted by miR-26a. *Pten* and *Stk11*, two genes involved in the PI3K-Akt signaling pathway; while *Hmga1*, *Rb1*, and ADAM Metalloproteinase Domain 17 (*Adam17*) for their role in adipogenesis were selected to confirm by real time PCR the downregulation induced by miR-26a mimic transfection at day 2 and 8. Furthermore, analysis of the impact induced by miR-26a inhibitor was also characterized in both stages of adipocyte differentiation (Figure 4). As expected, at day 2 of differentiation, the pre-adipocyte cells transfected with miR-26a mimic displayed lower expression of the target genes compared to the transfection control. Then, at day 8, a general trend of decreased mRNA expression was still observed, but differences only remained statistically significant for *Hmga1* (50%, $p = .003$) and *Stk11* (50%, $p = .010$). In addition, transfection with the inhibitor of miR-26a was associated with higher mRNA levels of *Rb1* (74%, $p = .040$) (day 2) and a tendency to greater expression of both *Adam17* ($p = .059$) and *Hmga1* ($p = .088$). No differences were observed at day 8 in cells transfected with the inhibitor. Therefore, the five selected genes were confirmed as reliable target genes for miR-26a action from starting stages of adipocyte differentiation in vitro and with potential influence on differentiated cells.

3.5 | Functional validation of miR-26a impact on target genes in adipose tissue of the offspring of cafeteria-fed dams

miR-26a expression in mammary gland was reduced (41.5%) in the cafeteria-fed dams compared with controls, which is in accordance with the lower levels of miR-26a in breastmilk that cafeteria-fed dams show¹³ (Supporting Information Figure S2A). Taking into account the in vitro results and considering a potential long-lasting epigenetic effect in vivo, we assessed whether target genes of miR-26a would be upregulated in the offspring of cafeteria-fed

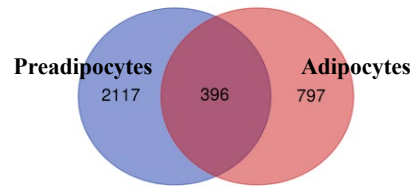
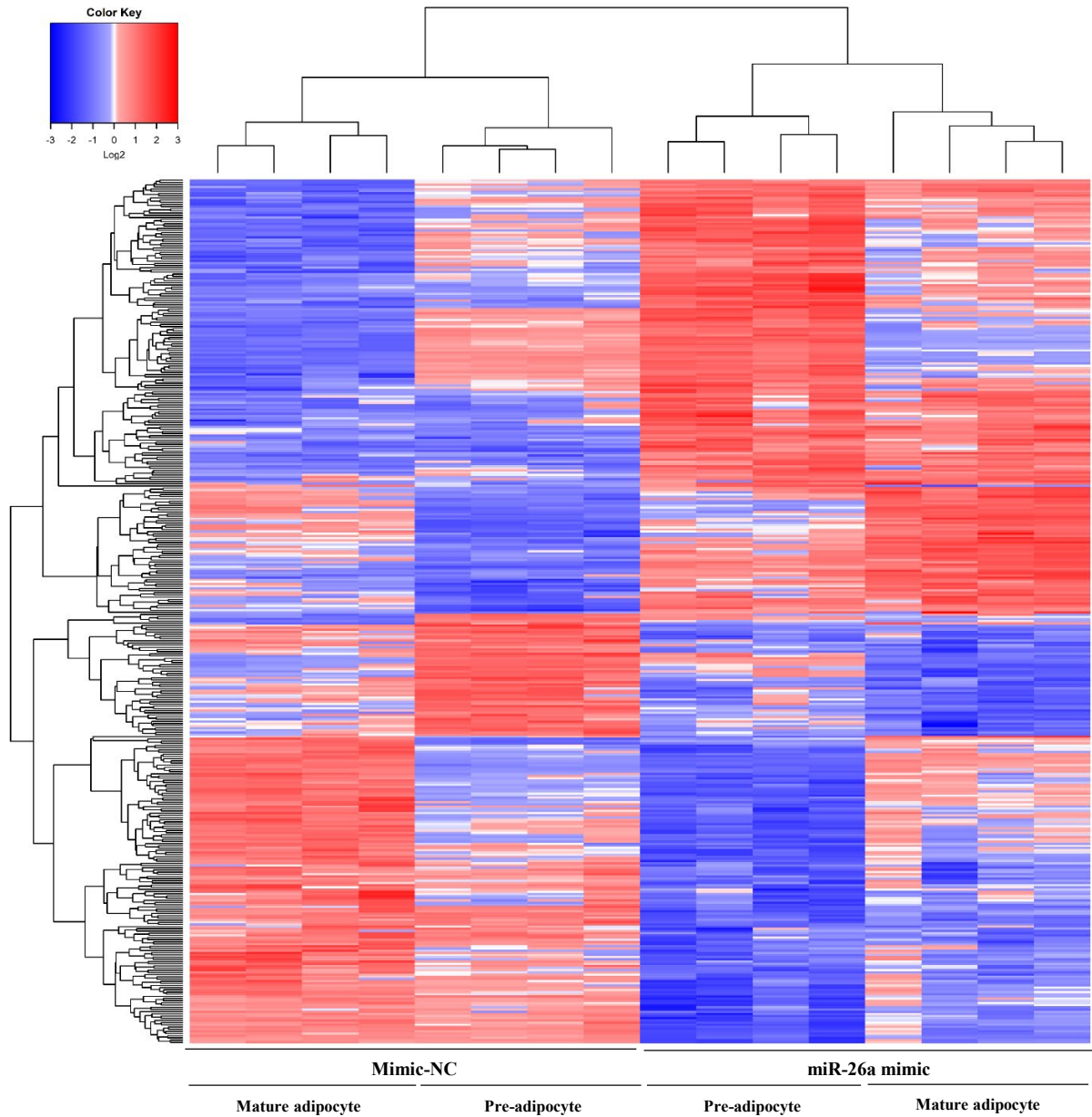
(A) Venn diagrams of altered target genes in miR-26a transfected cells**(B) Heat-map with altered target genes in miR-26a transfected cells**

FIGURE 3 Effect of miR-26a mimic transfection on mRNA expression in pre- and mature 3T3-L1 adipocytes. (A) Venn diagram comparing genes altered in miR-26a transfected cells and negative controls in both states of differentiation (Venn diagram was made in website <http://bioinformatics.psb.ugent.be/webtools/Venn/>). (B) Heat map of mRNA levels of genes altered in both states of differentiation. This heat map was constructed using R (v 3.3.1. R Development Core Team) and RStudio software after a range scaling method (zero-mean centered). The detailed list of genes can be found in Supporting Information Table S1

TABLE 1 List of predicted target genes downregulated in cells transfected with the miR-26a mimic in both stages of differentiation

Gene	Gene name	Preadipocyte		Adipocyte		Aggregate PCT	Pathway/Function
		logFC	Adj. p val.	logFC	Adj. p val.		
PTEN	Phosphatase and tensin homolog	-1.307	<.001	-0.939	.021	>0.99	Focal Adhesion-PI3K-Akt-mTOR-signaling pathway
LARP1	La ribonucleoprotein domain family, member 1	-1.055	<.001	-0.7193	.022	0.99	Cell proliferation
SLC25A16	Solute carrier family 25 (mitochondrial carrier; Graves disease autoantigen), member 16	-0.470	.013	-0.6397	.002	0.99	Metabolism of vitamins and cofactors
OTUD4	OTU domain containing 4	-1.121	<.001	-0.425	.009	0.98	Immune system process
UBN2	Ubinuclein 2	-0.363	.044	-0.5104	.006	0.98	Stem cell biology, development, and disease
KPNA6	Karyopherin alpha 6 (importin alpha 7)	-1.192	<.001	-0.6773	<.001	0.98	TNF-alpha NF-kB Signaling Pathway
ULK1	Unc-51 like autophagy activating kinase 1	-0.914	.002	-0.7486	.023	0.96	Focal Adhesion-PI3K-Akt-mTOR-signaling pathway
EPC2	Enhancer of polycomb homolog 2 (<i>Drosophila</i>)	-0.727	<.001	-0.4005	.008	0.96	Histone acetyltransferase activity
SNN	Stannin	-1.330	<.001	-0.7845	.007	0.95	Metal ion binding
SBNO1	Strawberry notch homolog 1 (<i>Drosophila</i>)	-1.005	<.001	-0.3332	.010	0.95	mRNA processing
CEP350	Centrosomal protein 350 kDa	-0.781	<.001	-0.4679	.041	0.94	Protein localization to centrosome
HMGA1	High mobility group AT-hook 1	-0.855	.005	-0.7393	.030	0.93	Adipogenesis genes
CHFR	Checkpoint with forkhead and ring finger domains, E3 ubiquitin protein ligase	-1.195	<.001	-0.7388	<.001	0.93	Cell cycle
LARP4B	La ribonucleoprotein domain family, member 4B	-0.778	<.001	-0.5408	<.001	0.93	Regulation of translation
TMEM184B	Transmembrane protein 184B	-0.696	<.001	-0.5105	.004	0.93	Transport
IPPK	Inositol 1,3,4,5,6-pentakisphosphate 2-kinase	-1.098	<.001	-0.6302	.038	0.92	Inositol phosphate metabolism
SRP19	Signal recognition particle 19 kDa	-0.987	<.001	-0.4887	.002	0.92	mRNA processing
NUP50	Nucleoporin 50 kDa	-0.869	<.001	-0.56	.020	0.92	Cell Cycle
BAK1	BCL2-antagonist/killer 1	-0.815	<.001	-0.3815	.014	0.91	Apoptosis
CPSF2	Cleavage and polyadenylation specific factor 2, 100 kDa	-0.801	.001	-0.5952	.031	0.9	mRNA processing
PCNX	Pecanex homolog (<i>Drosophila</i>)	-0.672	<.001	-0.3856	.034	0.89	Biological process
LN2	Ligand of numb-protein X 2	-0.360	.030	-0.4703	.007	0.87	Metal ion binding
ZBTB18	Zinc finger and BTB domain containing 18	-0.506	.007	-0.4873	.018	0.85	Regulation of transcription by RNA polymerase II
LSM12	LSM12 homolog (<i>S. cerevisiae</i>)	-1.164	.000	-0.3767	.045	0.84	Molecular function
OSBPL11	Oxysterol binding protein-like 11	-0.617	.0026	-0.6637	.003	0.81	Lipid transport
MKNK2	MAP kinase interacting serine/threonine kinase 2	-0.955	.002	-0.7121	.045	0.76	Intracellular signal transduction
TMEM68	Transmembrane protein 68	-0.420	.0035	-0.3857	.016	0.76	Biological process

(Continues)

TABLE 1 (Continued)

Gene	Gene name	Preadipocyte		Adipocyte		Aggregate PCT	Pathway/Function
		logFC	Adj. p val.	logFC	Adj. p val.		
SAR1B	SAR1 homolog B (<i>S. cerevisiae</i>)	-0.633	.000	-0.3354	.008	0.74	Immune System
FBXO28	F-box protein 28	-0.653	.000	-0.3126	.006	0.74	Protein polyubiquitination
CHD1	Chromodomain helicase DNA binding protein 1	-0.671	.0001	-0.4763	.013	0.74	Chromatin remodeling
ARFGEF1	ADP-ribosylation factor guanine nucleotide-exchange factor 1 (brefeldin A-inhibited)	-0.546	.0009	-0.435	.018	0.74	Golgi organization
ARL6IP6	ADP-ribosylation-like factor 6 interacting protein 6	-0.620	.000	-0.4099	<.001	0.73	Protein binding
FAM118A	Family with sequence similarity 118, member A	-0.533	.0011	-0.5397	.002	0.73	Protein binding
DNAJA2	DnaJ (Hsp40) homolog, subfamily A, member 2	-1.006	.000	-0.3047	.038	0.73	Cellular responses to external stimuli
WIPF2	WAS/WASL interacting protein family, member 2	-0.864	.000	-0.5421	.003	0.73	Actin filament-based movement
HNRNPUL1	Heterogeneous nuclear ribonucleoprotein U-like 1	-0.295	.0092	-0.4712	<.001	0.72	Metabolism of RNA
ARHGAP21	Rho GTPase activating protein 21	-0.396	.0004	-0.315	.010	0.7	Establishment of Golgi localization
MLEC	Malectin	-1.432	.000	-0.7378	.001	0.7	Carbohydrate metabolic process
RANBP9	RAN binding protein 9	-0.533	.0091	-0.6015	.006	0.68	Signaling by Receptor Tyrosine Kinases
YWHAE	Tyrosine 3-monooxygenase/tryptophan 5-monooxygenase activation protein, epsilon polypeptide	-0.468	.000	-0.3851	.001	0.68	Cell Cycle
MTPN	Myotrophin	-1.422	.000	-0.6505	<.001	0.6	Regulation of cell size
STK11	Serine/threonine kinase 11	-0.362	.0311	-0.4299	.017	0.57	Focal Adhesion-PI3K-Akt-mTOR-signaling pathway
FAM214B	Family with sequence similarity 214, member B	-0.989	.000	-0.5265	.004	0.56	Protein binding
ZCCHC2	Zinc finger, CCHC domain containing 2	-0.424	.0036	-0.5231	.001	0.55	Biological process
TXNDC15	Thioredoxin domain containing 15	-0.632	.0007	-0.5234	.011	0.49	Carbohydrate metabolism
INTU	Inturned planar cell polarity protein	-0.900	.003	-0.954	.004	0.49	Negative regulation of cell division
DCBLD1	Discoidin, CUB and LCCL domain containing 1	-0.532	.002	-0.3953	.047	0.39	Zymogen activation
REEP4	Receptor accessory protein 4	-1.020	.000	-0.5755	.030	0.38	Cell cycle
RB1	Retinoblastoma 1	-0.465	.0001	-0.5206	<.001	0.37	Adipogenesis genes
ATPAF1	ATP synthase mitochondrial F1 complex assembly factor 1	-1.059	.000	-0.3997	.024	0.33	Mitochondrial proton-transporting ATP synthase complex assembly

Note: Aggregate PCT, which ranges between 0 and 1, corresponds to a Bayesian estimate of the probability that a site conserved to a particular branch length is conserved due to miRNA targeting. The two most relevant functions in the context of this study are indicated in bold.

TABLE 2 Twenty-five signaling pathways affected in both pre- and mature adipocytes and identified with HiPathia analysis

ID	Name	Preadipocytes		Mature adipocyte	
		logFC	Adj. <i>p</i> val.	logFC	Adj. <i>p</i> val.
P-mmu04012-21	ErbB signaling pathway: Gsk3b	−0.014	<.001	−0.008	.012
P-mmu04012-25	ErbB signaling pathway: Cdkn1b	−0.013	.001	−0.010	.016
P-mmu04012-29	ErbB signaling pathway: Stat5a	0.031	.010	0.034	.010
P-mmu04022-23	cGMP-PKG signaling pathway: Cacna1c	−0.001	.015	−0.001	.001
P-mmu04022-44	cGMP-PKG signaling pathway: Bad	0.023	.024	0.036	.001
P-mmu04022-45	cGMP-PKG signaling pathway: Atf2	0.021	.017	0.032	.001
P-mmu04022-48	cGMP-PKG signaling pathway: Slc8a2	0.011	.020	0.022	<.001
P-mmu04022-49	cGMP-PKG signaling pathway: Atp1a1	0.021	.015	0.031	.001
P-mmu04022-50	cGMP-PKG signaling pathway: Atp2b2	0.012	.034	0.022	<.001
P-mmu04064-136	NF-kappa B signaling pathway: Tnfsf13b	−0.017	.040	−0.020	.033
P-mmu04151-100	PI3K-Akt signaling pathway: Prkca	0.013	<.001	0.010	.001
P-mmu04151-101	PI3K-Akt signaling pathway: Pkn2	0.009	.012	0.009	.036
P-mmu04151-102	PI3K-Akt signaling pathway: Sgk3	0.009	<.001	0.005	.017
P-mmu04151-4	PI3K-Akt signaling pathway: 105244208	0.010	<.001	0.007	.003
P-mmu04151-5	PI3K-Akt signaling pathway: Eif4b	0.007	.001	0.006	.010
P-mmu04330-19	Notch signaling pathway: Dtx1	0.003	.031	0.004	.041
P-mmu04610-45	Complement and coagulation cascades: C4b	0.013	.040	0.028	<.001
P-mmu04621-97	NOD-like receptor signaling pathway: Irf7	−0.010	.020	−0.012	.010
P-mmu04668-138	TNF signaling pathway: Nfkb1	−0.001	.002	−0.001	.010
P-mmu05169-104	Epstein-Barr virus infection: Irf3	−0.009	.007	−0.014	<.001
P-mmu05200-200	Pathways in cancer: Vegfd	−0.014	.034	−0.018	.012
P-mmu05200-202	Pathways in cancer: Vegfd	−0.014	.016	−0.013	.039
P-mmu05200-220	Pathways in cancer: Csf1r	0.032	.028	0.051	.001
P-mmu05215-43	Prostate cancer: Phosphatidylinositol-3,4,5-trisphosphate	−0.070	.001	−0.054	.018
P-mmu05230-100	Central carbon metabolism in cancer: Pten	−0.050	<.001	−0.040	<.001

dams (O-CAF) compared with the respective controls (O-C). At postnatal day 22, retroperitoneal adipose tissue showed higher expression of *Hmag1* (20%, $p = .016$), *Rb1* (30%, $p < .001$), and *Adam17* (19%, $p = .008$) in O-CAF animals in comparison with animals nursed by control-fed dams (O-C) (Figure 5), despite the fact that after weaning no differences regarding miR-26a expression in offspring adipose tissue were observed (Supporting Information Figure S2B). The data demonstrate the in vivo impact of suboptimal maternal miR-26a milk supply, action that might not be direct on miR-26a itself but on target mRNAs in adipose cells. However, the experimental set-up did not allow to discriminate the origin of miRNA, either from a source exogenous (eg milk) or made from endogenous synthesis (in offspring's adipose). Therefore, we cannot rule out a compensatory mechanism in offspring adipose increasing endogenous synthesis of miR-26a to compensate for lower milk supply or a temporal window of specific action. Nevertheless, these data are in close concordance

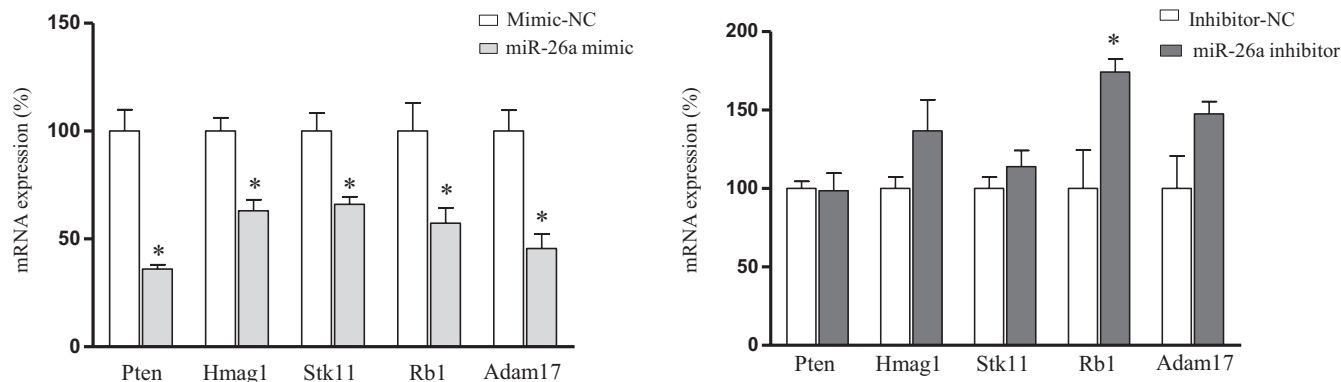
with the results obtained with in vitro transfection with either miR-26a mimic or inhibitor. Altogether, results support the physiological role of milk miRNAs for the progeny and their long-lasting impact in the adipose tissue of the offspring.

4 | DISCUSSION

The offspring of dams fed a cafeteria-diet show greater adiposity and related metabolic alterations.¹² In a previous paper, we demonstrated that miR-26a levels in breastmilk are sensitive to dietary intervention with an obesogenic diet during lactation.¹³ However, breastmilk from cafeteria-fed dams also differs in the levels of miR-222 and miR-200a, in the composition of macronutrients and on the concentration of bioactive peptides (such as leptin or adiponectin).^{12,13,26} Therefore, the current follow-up study conducted in the offspring of these animals contributed to

Target genes of miR-26a

(A) Pre-adipocyte cells (day 2)



(B) Differentiated adipocyte cells (day 8)

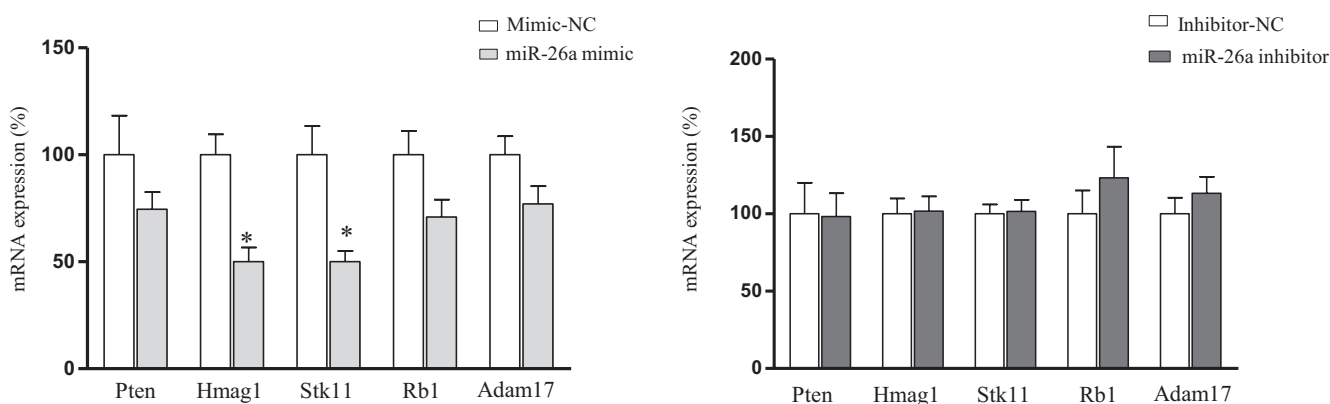


FIGURE 4 Effects of the mimic or inhibitor of miR-26a on the expression level of *Pten*, *Hmag1*, *Stk11*, *Rb1*, and *Adam17*. mRNA levels were measured by RT-qPCR and expressed as a percentage of the value of negative control cells on day 2 (A) and day 8 (B) after transfection. Data are mean \pm SEM from three separate experiments ($n = 6-10$). Statistics: *different versus control cells ($p < .05$, Mann-Whitney U test)

understand the impact of breastmilk with a composition modulated by maternal diet. However, offspring sample analysis did not allow to establish a direct cause-effect relationship with miR-26a or to rule out the contribution of other milk factors in the gene expression of target genes in offspring. Nevertheless, the in vitro approach, focused on determining the effect of miR-26a on the differentiation of adipocytes and the identification of its target genes by transcriptomic analysis has made it possible to specifically circumscribe the role of miR-26a and investigate whether lower levels in breastmilk could dysregulate the expression of genes linked to the developmental program of adipose tissue and account for impaired metabolic imprinting in the offspring. Altogether, both in vivo and in vitro data are complementary and suggest potential transgenerational effects mediated by miR-26a intervention.

From a mechanistic point of view, one miRNA may simultaneously control multiple effector genes binding to

the 3'-UTR sequence of their target mRNAs and inducing their degradation or slowing down the synthesis of the coded protein. miR-26 is a highly conserved family of vertebrate miRNAs transcribed from three genomic loci: miR-26a-1, miR-26a-2, and miR-26b.²⁷ This family plays a significant role in growth, development, and cell type specification,^{17,28-30} with growing evidence supporting its relevance in adipocyte differentiation.^{17,31} miR-26a and miR-26b share nearly identical sequences, and probably function redundantly.²¹ Specifically, during human adipogenesis, miR-26a is induced early on and is required for its progression; its inhibition has a pronounced negative effect on adipocyte differentiation whereas its overexpression has the opposite effect.¹⁷ Similarly, miR-26b expression gradually increases to a stable level during human pre-adipocyte differentiation, its inhibition suppresses differentiation, and its overexpression accelerates the induction of adipogenic markers and increases lipid

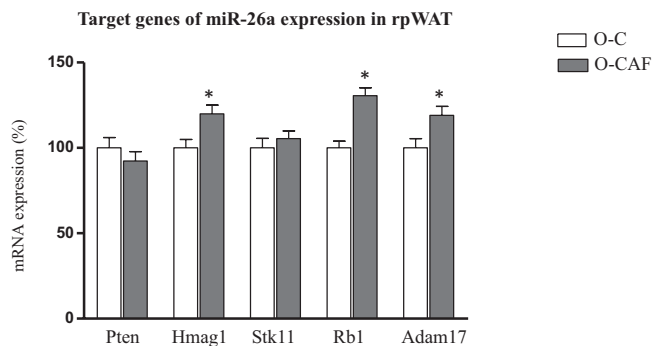


FIGURE 5 Expression of target genes (*Pten*, *Hmg1*, *Stk11*, *Rb1*, and *Adam17*) of miR-26a in retroperitoneal white adipose tissue of the offspring of control and cafeteria fed dams during lactation on postnatal 22 (PN22). Data are mean \pm SEM of 16–20. Statistics: *different versus control animals ($p < .05$, Student's *t*-test)

accumulation.^{18,31} Interestingly, obese subjects and animal models of obesity are characterized by reduced levels of miR-26b in visceral adipose tissue, which is related to metabolic dysfunction and insulin resistance.²⁰ Therefore, lower levels of miR-26a in breastmilk are in agreement with this scenario and suggest its involvement in the induction of a metabolic imprinting program channeled by maternal milk toward the progeny.

Transcriptomic data from the *in vitro* assay in 3T3-L1 cells, promoting overexpression of miR-26a, identified a number of genes influenced at an early stage of differentiation up to mature adipocytes. Moreover, 396 genes were altered in both states of differentiation. Fifty of these were downregulated and contained multiple conserved predicted miR-26a binding sites, thus making them the most likely direct target genes of miR-26a. Further comprehensive analyses pointed out the relevance of miR-26a targets involved in PI3K-Akt pathway, represented by *Pten* and *Stk11*; those involved with adipogenesis (*Hmg1*, *Adam17*, and *Rb1*); and those with related functions (lipid transport, cell cycle, and regulation of cell size). Specifically, we further characterized and confirmed the role of these five genes during the adipogenesis progress both *in vitro* and *in vivo* and the results give support to their involvement in early adipocyte metabolic programming and obesity development.

Microarray screening with a partial number of samples suggested that *Pten* was a target of miR-26a, which was further confirmed with the validation analysis by PCR in the whole set of samples. The results fit with the redundancy observed for the miR-26 family, as *PTEN* has been described as a direct target for miR-26b.³¹ *PTEN* dephosphorylates phosphatidylinositol-3,4,5-phosphate (PIP3), thereby inhibiting the activation of downstream proteins in the PI3K pathway (reviewed in Ref. [32]). Therefore, as

seen with miR-26a mimic in the transfection approach, *Pten* decrease might upregulate PI3K signaling and downstream proteins including the serine/threonine kinase AKT and protein kinase C.¹⁸ This may have relevant consequences, as AKT plays a critical role in adipocyte differentiation and its inhibition blocks the differentiation of 3T3-L1 cells.^{33,34} Furthermore, mouse embryonic fibroblasts lacking Akt1 display an inability to differentiate into adipocytes.^{35,36} Interestingly, the PIK3-AKT signaling pathway was one of the most permanently affected in 3T3-L1 pre- and mature adipocytes transfected with the miR-26a mimic at early stages of differentiation. Our results are in accordance with the activation of this signaling pathway that would be mediated by miR-26a through binding to 3'UTR of *Pten*. Although no cause-effect relationship can be established with the current data, miR-26a could promote 3T3-L1 cell differentiation via targeting *Pten*¹⁸ and, thus, result in an upregulation of the AKT pathway.

In close connection with the above, *Stk11* was also downregulated in cells transfected with the miR-26a mimic in both states of differentiation. STK11 signaling keeps adipocyte progenitors in their non-differentiated stage.³⁷ Silencing or knockout of *Stk11* in 3T3-L1 preadipocytes or mouse embryonic fibroblasts upregulates the expression of *Cebp α* and *Ppar γ* , promoting lipid accumulation and differentiation to mature adipocytes.³⁷ On the other hand, 3T3-L1 adipocytes overexpressing *Stk11* show a browning phenotype.³⁸ Although transfection with the miR-26a mimic led to downregulation of both *Pten* and *Stk11* and confirmed them as targets of miR-26a, as well as the expected metabolic consequences which would favor preadipocyte differentiation and adipogenesis, no impact on *Pten* or *Stk11* expression was observed in cells transfected with the miR-26a inhibitor or in the animal model breastfed with a lower concentration of miR-26a. In general, transfection with the inhibitor accounted for smoother effects on gene expression than those seen with the mimic, suggesting that a higher dose was needed in order to counteract the action of the internal miR-26a, or the fact that underlying compensatory mechanisms were present. Furthermore, the observed lack of impact on the gene expression of these two target genes in animals at 22 days seems to support the latter scenario, as the lower levels of miR-26a in breastmilk contributed to the early metabolic programming of obesity.¹²

In fact, the expression of the three other genes characterized (*Hmg1*, *Rb1*, and *Adam17*) contributed to confirm this hypothesis. *HMGA1* (also known as *HMG1/Y*), which regulates chromatin structure and gene transcription, contains a 3'-UTR sequence for miR-26a. *Hmg1* expression was downregulated in both states of cell differentiation when transfected with the mimic, in accordance with the proposal that miR-26, among other miRNAs,

may bind HMGA1 and increase its degradation or block its translation.³⁹ Concerning its role during development, *Hmga1* is highly expressed in the early stages of development in both white and brown adipose tissues in mice and, during adulthood, decreases steadily to plateau levels.⁴⁰ The adipocyte-specific overexpression of *Hmga1* in transgenic mice results in impaired development of white and brown adipose tissues through the inhibition of the adipogenic process, resulting in increased adipose precursor pool populations.⁴⁰ In agreement with the *in vitro* results, *in vivo* data showed that *Hmga1* mRNA levels were upregulated in the adipose tissue of the offspring of dams with lower levels of miR-26a in breastmilk. This early alteration on *Hmga1* could be, to some extent, responsible for the specific programming driving to the long-term dysmetabolic consequences found in these animals; they present a greater fat mass and impaired response to OGTT in adulthood.¹² In fact, HMGA1 is crucial for the transcriptional regulation of genes involved in glucose metabolism, including the insulin receptor (INSR) (reviewed in⁴¹). The interaction of insulin with its receptor induces the phosphorylation of HMGA1 via AKT, and induces INSR transcriptional repression.⁴² In this way, HMGA1 can play a role as a molecular switch deactivating/activating INSR protein expression during fed/fasting conditions.⁴² Therefore, milk miR-26a levels targeting *Hmga1* mRNA could contribute to adequately program insulin signaling and glucose metabolism regulation in the nursed progeny. The lower intake of miR-26a mediated by breastfeeding with cafeteria diet-fed dams increased the expression of *Hmga1* in white adipose tissue of the offspring and, consequently, altered its regulatory and metabolic programming role, which could be responsible for the dysregulated insulin signaling pathway.¹²

The levels of *Rb1* mRNA were also downregulated in cells transfected with the mimic of miR-26a in pre-adipocytes and, to a lesser extent, in mature adipocytes. In addition, *Rb1* expression increased in cells transfected with the inhibitor of miR-26a and in the adipose tissue of the offspring of cafeteria-fed dams. *Rb1* encodes the retinoblastoma protein that is a nuclear phosphoprotein regulator of the cell cycle through binding to the E2F family of transcription factors and preventing them from activating the genes required for G1/S phase progression.^{43,44} In addition to cell cycle control, our group was the first to suggest its involvement in adipocyte differentiation.⁴⁵ Nevertheless, changes in the expression of *Rb1* may show dissimilar outcomes. On the one hand, the inactivation or deletion of *Rb* in adipose tissues leads to anti-obesity outcomes in a mouse model of diet-induced obesity.⁴⁶⁻⁴⁸ In this sense, pRb haploinsufficiency also protects against diet-induced obesity and associated metabolic disturbances in mice.⁴⁸ On the other hand, rats fed during 16 weeks with

obesogenic cafeteria diet show decreased expression of *Rb* in white fat depots at both mRNA and protein levels⁴⁹; in agreement, adipose tissues of obese subjects, have lower RB expression (mRNA and protein) than normo-weight subjects.⁴⁹ RB1 is able to activate C/EBP α -mediated transcription which leads to adipocyte differentiation.^{50,51} Thus, the lower levels of miR-26a supplied by maternal milk would favor greater mRNA expression of *Rb1* at an early age, when adipose tissue is developing, which could favor clonal expansion and differentiation and the increase in fat mass observed in these animals.

Finally, the miR-26 family reduces the activity of *Adam17*, possibly through physical interaction with its 3'-UTR.¹⁷ In accordance with this, repressed expression of *Adam17* mRNA was observed in pre-adipocytes of 3T3-L1 cells transfected with the miR-26a mimic. Moreover, the offspring of cafeteria dams that had a lower supply of miR-26a through breastmilk displayed a greater mRNA expression of *Adam17* compared to controls. ADAM17 cleaves the membrane-bound TNF α precursor to generate its soluble and mature form^{52,53} and other membrane-anchored proteins.⁵⁴ ADAM17 activity is higher in liver, white adipose tissue, and muscle of animals fed a high-fat diet.⁵⁵ ADAM17 activation may contribute to the development of metabolic disorders⁵⁶ and, in liver, its activation contributes to the development of non-alcoholic fatty liver disease.⁵⁵ However, haplo-insufficient mice are protected against diet-induced obesity and insulin resistance.⁵⁷ Interestingly, a temporal systemic deletion of ADAM17 protects against body weight gain induced by high-fat diet, insulin resistance, and hepatosteatosis.⁵⁸ Therefore, modulation of ADAM17 activity could act against obesity and its metabolic complications. Thus, the lower milk-born miR-26a levels associated with maternal intake of an obesogenic diet alters the mechanism that modulates the expression of *Adam17*, and its induction may contribute to the obese phenotype observed in the animals.

All in all, mice lacking the highly conserved miR-26 miRNA family present a dramatic expansion of adipose tissue early in adult life.²¹ Therefore, the greater fat mass observed in the offspring of cafeteria fed dams, already present at early age, could be due, at least in part, to the lower miR-26a supply through breastmilk in these animals. To further study the hypothesis, a first approach was set up *in vitro* with the widely used adipocyte differentiation model system, the mouse 3T3-L1 pre-adipocyte cell line. This enabled the miR-26a target genes to be identified during growth and adipocyte differentiation and a representative sample to be selected upon confirmation of their role in the process of adipocyte development. Then, to assess the physiological relevance of a lower supply of miR-26a during lactation, target genes were determined

in adipose tissue of the offspring, obtaining results that supported the functional relationship between miR-26a and its impact on the expression of genes involved in adipogenesis and related functions like lipid transport, cell cycle, and regulation of cell size. Furthermore, results contribute to confirm that milk-derived miRNAs once consumed they can exert an effect on target mRNA in specific tissues of the consumers^{59–63}

Particularly, upregulation of the miR-26a target genes *Hmag1*, *Rb1*, and *Adam17* at transcript and/or protein level was associated with the development of obesity and related metabolic alterations. The results contribute to show the physiological relevance of miRNA in breastmilk for the lactating infant and its involvement in metabolic programming of obesity, as well as the relevance of maternal diet during lactation in the setting up of the programming conditions mediated by miRNAs. We describe here that lower levels of miR-26a in breastmilk might alter the early expression of target genes in offspring and be related to adverse metabolic programming effects at an early age and tentatively remaining in adulthood. In conclusion, given the role of the miR-26a family and their target genes in core metabolic homeostasis processes, the transfer of miR-26a through milk could constitute a potential mechanism by which maternal diet can modulate offspring adipose tissue development and expansion, affecting obesity susceptibility in the infant and pointing toward the role of miR-26a as an epigenetic regulator.

ACKNOWLEDGMENTS

This research was supported by Project “PI17/01614”, funded by *Instituto de Salud Carlos III* and co-funded by European Union (ERDF/ESF, “Investing in your future”). The Research Group Nutrigenomics, Biomarkers and Risk Evaluation (NuBE) receives financial support from *Instituto de Salud Carlos III*, *Centro de Investigación Biomédica en Red Fisiopatología de la Obesidad y Nutrición*, CIBERobn, and is a member of the European Research Network of Excellence NuGO (The European Nutrigenomics Organization, EU Contract: no. FP6-506360).

DISCLOSURES

The authors declare that they have no conflict of interest.

AUTHOR CONTRIBUTIONS

Francisca Serra, Andreu Palou, and Juana Sánchez designed the research. Catalina A. Pomar, Francisca Serra, and Juana Sánchez analyzed the data. Catalina A. Pomar and Juana Sánchez performed the research. Catalina A. Pomar, Francisca Serra, Andreu Palou, and Juana Sánchez wrote the paper. All authors have revised the manuscript and approved the final version.

ORCID

Catalina A. Pomar  <https://orcid.org/0000-0002-8113-761X>

Francisca Serra  <https://orcid.org/0000-0002-8307-9732>

Andreu Palou  <https://orcid.org/0000-0002-0295-4452>

Juana Sánchez  <https://orcid.org/0000-0002-9176-8060>

REFERENCES

1. Armstrong J, Reilly JJ, Team CHI. Breastfeeding and lowering the risk of childhood obesity. *Lancet*. 2002;359(9322):2003–2004. doi:10.1016/S0140-6736(02)08837-2
2. Horta BL, Loret de Mola C, Victora CG. Long-term consequences of breastfeeding on cholesterol, obesity, systolic blood pressure and type 2 diabetes: a systematic review and meta-analysis. *Acta Paediatr*. 2015;104(467):30–37. doi:10.1111/apa.13133
3. Yan J, Liu L, Zhu Y, Huang G, Wang PP. The association between breastfeeding and childhood obesity: a meta-analysis. *BMC Public Health*. 2014;14:1267. doi:10.1186/1471-2458-14-1267
4. Jaenisch R, Bird A. Epigenetic regulation of gene expression: how the genome integrates intrinsic and environmental signals. *Nat Genet*. 2003;33(suppl):245–254. doi:10.1038/ng1089
5. Feinberg AP. Phenotypic plasticity and the epigenetics of human disease. *Nature*. 2007;447(7143):433–440. doi:10.1038/nature05919
6. Hochberg Z, Feil R, Constancia M, et al. Child health, developmental plasticity, and epigenetic programming. *Endocr Rev*. 2011;32(2):159–224. doi:10.1210/er.2009-0039
7. Weber JA, Baxter DH, Zhang S, et al. The microRNA spectrum in 12 body fluids. *Clin Chem*. 2010;56(11):1733–1741. doi:10.1373/clinchem.2010.147405
8. Melnik BC, Schmitz G. MicroRNAs: milk's epigenetic regulators. *Best Pract Res Clin Endocrinol Metab*. 2017;31(4):427–442. doi:10.1016/j.beem.2017.10.003
9. Munch EM, Harris RA, Mohammad M, et al. Transcriptome profiling of microRNA by Next-Gen deep sequencing reveals known and novel miRNA species in the lipid fraction of human breast milk. *PLoS ONE*. 2013;8(2):e50564. doi:10.1371/journal.pone.0050564
10. Xi Y, Jiang X, Li R, Chen M, Song W, Li X. The levels of human milk microRNAs and their association with maternal weight characteristics. *Eur J Clin Nutr*. 2016;70(4):445–449. doi:10.1038/ejcn.2015.168
11. Zamanillo R, Sánchez J, Serra F, Palou A. Breast milk supply of microRNA associated with leptin and adiponectin is affected by maternal overweight/obesity and influences infancy BMI. *Nutrients*. 2019;11(11):2589. doi:10.3390/nu11112589
12. Pomar CA, van Nes R, Sánchez J, Picó C, Keijer J, Palou A. Maternal consumption of a cafeteria diet during lactation in rats leads the offspring to a thin-outside-fat-inside phenotype. *Int J Obes*. 2017;41(8):1279–1287. doi:10.1038/ijo.2017.42
13. Pomar CA, Castro H, Picó C, Serra F, Palou A, Sánchez J. Cafeteria diet consumption during lactation in rats, rather than obesity per se, alters miR-222, miR-200a, and miR-26a levels in milk. *Mol Nutr Food Res*. 2019;63(8):e1800928. doi:10.1002/mnfr.201800928
14. Xie H, Lim B, Lodish HF. MicroRNAs induced during adipogenesis that accelerate fat cell development are downregulated in obesity. *Diabetes*. 2009;58(5):1050–1057. doi:10.2337/db08-1299
15. Son YH, Ka S, Kim AY, Kim JB. Regulation of adipocyte differentiation via microRNAs. *Endocrinol Metab*. 2014;29(2):122–135. doi:10.3803/EnM.2014.29.2.122

16. Hilton C, Neville MJ, Karpe F. MicroRNAs in adipose tissue: their role in adipogenesis and obesity. *Int J Obes*. 2013;37(3):325-332. doi:10.1038/ijo.2012.59
17. Karbiener M, Pisani DF, Frontini A, et al. MicroRNA-26 family is required for human adipogenesis and drives characteristics of brown adipocytes. *Stem Cells*. 2014;32(6):1578-1590. doi:10.1002/stem.1603
18. Li G, Ning C, Ma Y, et al. miR-26b promotes 3T3-L1 adipocyte differentiation through targeting PTEN. *DNA Cell Biol*. 2017;36(8):672-681. doi:10.1089/dna.2017.3712
19. Fu X, Dong B, Tian Y, et al. MicroRNA-26a regulates insulin sensitivity and metabolism of glucose and lipids. *J Clin Invest*. 2015;125(6):2497-2509. doi:10.1172/JCI175438
20. Xu G, Ji C, Song G, et al. MiR-26b modulates insulin sensitivity in adipocytes by interrupting the PTEN/PI3K/AKT pathway. *Int J Obes*. 2015;39(10):1523-1530. doi:10.1038/ijo.2015.95
21. Acharya A, Berry DC, Zhang H, et al. miR-26 suppresses adipocyte progenitor differentiation and fat production by targeting. *Genes Dev*. 2019;33(19-20):1367-1380. doi:10.1101/gad.328955.119
22. Pomar CA, Kuda O, Kopecky J, et al. Maternal diet, rather than obesity itself, has a main influence on milk triacylglycerol profile in dietary obese rats. *Biochim Biophys Acta Mol Cell Biol Lipids*. 2020;1865(2):158556. doi:10.1016/j.bbalip.2019.158556
23. Hidalgo MR, Cubuk C, Amadoz A, Salavert F, Carbonell-Caballero J, Dopazo J. High throughput estimation of functional cell activities reveals disease mechanisms and predicts relevant clinical outcomes. *Oncotarget*. 2017;8(3):5160-5178. doi:10.18632/oncotarget.14107
24. Dykxhoorn DM, Novina CD, Sharp PA. Killing the messenger: short RNAs that silence gene expression. *Nat Rev Mol Cell Biol*. 2003;4(6):457-467. doi:10.1038/nrm1129
25. Friedman RC, Farh KK, Burge CB, Bartel DP. Most mammalian mRNAs are conserved targets of microRNAs. *Genome Res*. 2009;19(1):92-105. doi:10.1101/gr.082701.108
26. Pomar CA, Sánchez J, Palou A. The intake of a cafeteria diet in nursing rats alters the breast milk concentration of proteins important for the development of offspring. *Nutrients*. 2020;12(8):2470. doi:10.3390/nu12082470
27. Gao J, Liu QG. The role of miR-26 in tumors and normal tissues (Review). *Oncol Lett*. 2011;2(6):1019-1023. doi:10.3892/ol.2011.413
28. Dey BK, Gagan J, Yan Z, Dutta A. miR-26a is required for skeletal muscle differentiation and regeneration in mice. *Genes Dev*. 2012;26(19):2180-2191. doi:10.1101/gad.198085.112
29. Trompeter H-I, Dreesen J, Hermann E, et al. MicroRNAs miR-26a, miR-26b, and miR-29b accelerate osteogenic differentiation of unrestricted somatic stem cells from human cord blood. *BMC Genom*. 2013;14:111. doi:10.1186/1471-2164-14-111
30. Dill H, Linder B, Fehr A, Fischer U. Intronic miR-26b controls neuronal differentiation by repressing its host transcript, ctdsp2. *Genes Dev*. 2012;26(1):25-30. doi:10.1101/gad.177774.111
31. Song G, Xu G, Ji C, et al. The role of microRNA-26b in human adipocyte differentiation and proliferation. *Gene*. 2014;533(2):481-487. doi:10.1016/j.gene.2013.10.011
32. Chen CY, Chen J, He L, Stiles BL. PTEN: tumor suppressor and metabolic regulator. *Front Endocrinol*. 2018;9:338. doi:10.3389/fendo.2018.00338
33. Xu J, Liao K. Protein kinase B/AKT 1 plays a pivotal role in insulin-like growth factor-1 receptor signaling induced 3T3-L1 adipocyte differentiation. *J Biol Chem*. 2004;279(34):35914-35922. doi:10.1074/jbc.M402297200
34. Zhang HH, Huang J, Düvel K, et al. Insulin stimulates adipogenesis through the Akt-TSC2-mTORC1 pathway. *PLoS ONE*. 2009;4(7):e6189. doi:10.1371/journal.pone.0006189
35. Peng XD, Xu PZ, Chen ML, et al. Dwarfism, impaired skin development, skeletal muscle atrophy, delayed bone development, and impeded adipogenesis in mice lacking Akt1 and Akt2. *Genes Dev*. 2003;17(11):1352-1365. doi:10.1101/gad.1089403
36. Yun SJ, Kim EK, Tucker DF, Kim CD, Birnbaum MJ, Bae SS. Isoform-specific regulation of adipocyte differentiation by Akt/protein kinase B α . *Biochem Biophys Res Commun*. 2008;371(1):138-143. doi:10.1016/j.bbrc.2008.04.029
37. Gormand A, Berggreen C, Amar L, et al. LKB1 signalling attenuates early events of adipogenesis and responds to adipogenic cues. *J Mol Endocrinol*. 2014;53(1):117-130. doi:10.1530/JME-13-0296
38. Xi P, Xue J, Wu Z, et al. Liver kinase B1 induces browning phenotype in 3 T3-L1 adipocytes. *Gene*. 2019;682:33-41. doi:10.1016/j.gene.2018.10.012
39. D'Angelo D, Esposito F, Fusco A. Epigenetic mechanisms leading to overexpression of HMGA proteins in human pituitary adenomas. *Front Med*. 2015;2:39. doi:10.3389/fmed.2015.00039
40. Arce-Cerezo A, García M, Rodríguez-Nuevo A, et al. HMGA1 overexpression in adipose tissue impairs adipogenesis and prevents diet-induced obesity and insulin resistance. *Sci Rep*. 2015;5:14487. doi:10.1038/srep14487
41. Chiefari E, Foti DP, Sgarra R, et al. Transcriptional regulation of glucose metabolism: the emerging role of the HMGA1 chromatin factor. *Front Endocrinol*. 2018;9:357. doi:10.3389/fendo.2018.00357
42. Chiefari E, Nevo MT, Arcidiacono B, et al. HMGA1 is a novel downstream nuclear target of the insulin receptor signaling pathway. *Sci Rep*. 2012;2:251. doi:10.1038/srep00251
43. Frolov MV, Dyson NJ. Molecular mechanisms of E2F-dependent activation and pRB-mediated repression. *J Cell Sci*. 2004;117(pt 11):2173-2181. doi:10.1242/jcs.01227
44. Sage J, Miller AL, Pérez-Mancera PA, Wysocki JM, Jacks T. Acute mutation of retinoblastoma gene function is sufficient for cell cycle re-entry. *Nature*. 2003;424(6945):223-228. doi:10.1038/nature01764
45. Puigserver P, Nadal-Ginard B, Palou A. Expression and interaction of C/EBP α adipogenic transcription factor and retinoblastoma protein in adipocytes during differentiation. *Int J Obes Relat Metab Disord*. 1994;18:113.
46. Dali-Youcef N, Matakis C, Coste A, et al. Adipose tissue-specific inactivation of the retinoblastoma protein protects against diabetes because of increased energy expenditure. *Proc Natl Acad Sci U S A*. 2007;104(25):10703-10708. doi:10.1073/pnas.0611568104
47. Petrov PD, Ribot J, Palou A, Bonet ML. Improved metabolic regulation is associated with retinoblastoma protein gene haploinsufficiency in mice. *Am J Physiol Endocrinol Metab*. 2015;308(2):E172-E183. doi:10.1152/ajpendo.00308.2014
48. Mercader J, Ribot J, Murano I, et al. Haploinsufficiency of the retinoblastoma protein gene reduces diet-induced obesity, insulin resistance, and hepatosteatosis in mice. *Am J Physiol Endocrinol Metab*. 2009;297(1):E184-E193. doi:10.1152/ajpen.2009.00163.2009
49. Moreno-Navarrete JM, Petrov P, Serrano M, et al. Decreased RB1 mRNA, protein, and activity reflect obesity-induced

- altered adipogenic capacity in human adipose tissue. *Diabetes*. 2013;62(6):1923-1931. doi:10.2337/db12-0977
50. Puigserver P, Ribot J, Serra F, et al. Involvement of the retinoblastoma protein in brown and white adipocyte cell differentiation: functional and physical association with the adipogenic transcription factor C/EBPalpha. *Eur J Cell Biol*. 1998;77(2):117-123. doi:10.1016/s0171-9335(98)80079-4
 51. Chen PL, Riley DJ, Chen Y, Lee WH. Retinoblastoma protein positively regulates terminal adipocyte differentiation through direct interaction with C/EBPs. *Genes Dev*. 1996;10(21):2794-2804. doi:10.1101/gad.10.21.2794
 52. Black RA, Rauch CT, Kozlosky CJ, et al. A metalloproteinase disintegrin that releases tumour-necrosis factor-alpha from cells. *Nature*. 1997;385(6618):729-733. doi:10.1038/385729a0
 53. Moss ML, Jin SL, Milla ME, et al. Cloning of a disintegrin metalloproteinase that processes precursor tumour-necrosis factor-alpha. *Nature*. 1997;385(6618):733-736. doi:10.1038/385733a0
 54. Blobel CP. ADAMs: key components in EGFR signalling and development. *Nat Rev Mol Cell Biol*. 2005;6(1):32-43. doi:10.1038/nrm1548
 55. Fiorentino L, Vivanti A, Cavalera M, et al. Increased tumor necrosis factor alpha-converting enzyme activity induces insulin resistance and hepatosteatosis in mice. *Hepatology*. 2010;51(1):103-110. doi:10.1002/hep.23250
 56. Menghini R, Fiorentino L, Casagrande V, Lauro R, Federici M. The role of ADAM17 in metabolic inflammation. *Atherosclerosis*. 2013;228(1):12-17. doi:10.1016/j.atherosclerosis.2013.01.024
 57. Serino M, Menghini R, Fiorentino L, et al. Mice heterozygous for tumor necrosis factor-alpha converting enzyme are protected from obesity-induced insulin resistance and diabetes. *Diabetes*. 2007;56(10):2541-2546. doi:10.2337/db07-0360
 58. Kaneko H, Anzai T, Horiuchi K, et al. Tumor necrosis factor- α converting enzyme inactivation ameliorates high-fat diet-induced insulin resistance and altered energy homeostasis. *Circ J*. 2011;75(10):2482-2490. doi:10.1253/circj.cj-11-0182
 59. Izumi H, Kosaka N, Shimizu T, Sekine K, Ochiya T, Takase M. Bovine milk contains microRNA and messenger RNA that are stable under degradative conditions. *J Dairy Sci*. 2012;95(9):4831-4841. doi:10.3168/jds.2012-5489
 60. Alsaweed M, Hartmann PE, Geddes DT, Kakulas F. MicroRNAs in breastmilk and the lactating breast: potential immunoprotectors and developmental regulators for the infant and the mother. *Int J Environ Res Public Health*. 2015;12(11):13981-14020. doi:10.3390/ijerph121113981
 61. Melnik BC, John SM, Schmitz G. Milk: an exosomal microRNA transmitter promoting thymic regulatory T cell maturation preventing the development of atopy? *J Transl Med*. 2014;12:43. doi:10.1186/1479-5876-12-43
 62. Baier SR, Nguyen C, Xie F, Wood JR, Zemleni J. MicroRNAs are absorbed in biologically meaningful amounts from nutritionally relevant doses of cow milk and affect gene expression in peripheral blood mononuclear cells, HEK-293 kidney cell cultures, and mouse livers. *J Nutr*. 2014;144(10):1495-1500. doi:10.3945/jn.114.196436
 63. McNeill EM, Hirschi KD. Roles of regulatory RNAs in nutritional control. *Annu Rev Nutr*. 2020;9(40):77-104. doi:10.1146/annurev-nutr-122319-035633

SUPPORTING INFORMATION

Additional Supporting Information may be found in the online version of the article at the publisher's website.

How to cite this article: Pomar CA, Serra F, Palou A, Sánchez J. Lower miR-26a levels in breastmilk affect gene expression in adipose tissue of offspring. *FASEB J*. 2021;35:e21924. <https://doi.org/10.1096/fj.202100623R>